

System Benefits for Solar Inverters using SiC Semiconductor Modules

Ulrich Schwarzer ulrich.schwarzer@infineon.com

Stefan Buschhorn stefan.buschhorn@infineon.com

Klaus Vogel klaus.vogel@infineon.com

Infineon Technologies AG, Max-Planck-Strasse 5, D-59581 Warstein, Germany

Abstract

In today's and future's electrical power grid system, regenerative energy sources like photovoltaic (PV) power systems consisting of PV panels and grid-connected inverters are very popular in domestic as well as in commercial power plants. High competitive pressure among PV power system providers due to cut inverter's costs can be observed. Therefore different technical approaches have to be evaluated in overall power inverter system cost to get cost-optimized solutions. In this paper technical and system cost benefits in a grid-connected, transformerless multi-string PV inverter box by replacing its standard silicon (Si) IGBT modules with fast switching silicon carbide (SiC) device modules will be shown and discussed.

1 Introduction

Many publications are in circulation highlighting the awesome properties of novel high power silicon carbide (SiC) devices and their technical advantages in different applications. Due to reduced switching losses and therefore increased switching frequency, generally the size of peripheral passive components can be minimized and / or conversion power efficiency can be improved, respectively.

The use of novel silicon carbide devices like SiC JFETs in PV solar inverter systems is often proposed to improve power density and power efficiency which are still unique selling points for PV solar plants.

Due to the technical production challenges and therefore relative high expenses of SiC devices, there is still the question, if the reduced share of expenses of passive components and housings legitimates the use of SiC devices in cost-sensitive PV solar inverter market.

In this paper, the cost-improving issues of a grid-connected PV solar inverter system will be highlighted and alternative, redesign solutions with SiC devices will be presented and explained. After that, the cost potentials of proposed redesign will be evaluated to indicate the system cost benefit in PV solar inverters using SiC devices.

2 Technical approaches of grid-connected PV solar plants

2.1 Overview

In [1] different topologies and power inverter types for grid-connected PV power plants, like string converter, solar panel with integrated AC inverter, central converter and multi-string converter are listed and compared.

Due to different voltage and power ratings of PV solar plants, the optimal solution of the different topologies has to be chosen to feed PV energy into the electric power grid with the maximum possible efficiency. The competition among the PV system suppliers to increase efficiency in the position after decimal point of 98% or even 99% has been shifted to cut down the inverter's costs. There are several technical approaches which will be discussed here.

Fulfilling the technical rules and standards, some power suppliers even allow solar plant users the operation of transformerless, directly grid-connected power converters to reach good efficiency [6]. One of the most popular and advantageous topologies is the transformerless grid-connected multi-string PV inverter.

The chosen multi-string topology and power range are widely used today to achieve high efficiency in home-based PV installations with an output power of typically $P_{out,N} = 10..30$ kW.

2.2 Focus: transformerless multi-string PV inverter

In Fig. 1 the block diagram of a typical multi-string transformerless grid-connected PV inverter system is depicted.

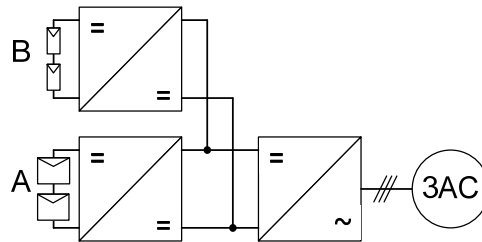


Fig. 1: Block diagram of a typical multi-string PV inverter system

In this example the PV system consists of an input terminal connecting two PV strings A and B with different input power range specifications. This is for independent and overall efficient PV generator operation: shadowed PV cells due to the PV power plant's non-optimal position between neighbored roofs during sunrise and/or sunset are connected to the smaller power input B while the main PV cell areas will provide the most power contingent to the larger power input A.

Both DC/DC converters (see Fig. 1) operate independently from each other and supply a common DC-link. To obtain optimal efficiency, DC/DC converters are operating under maximum power point tracking (MMPT) conditions. The DC/AC converter provides a sinusoidal three-phase AC current with grid frequency.

The circuit diagram of an exemplary multi-string PV solar inverter topology for the three-phase 400 V system is shown in Fig. 2.

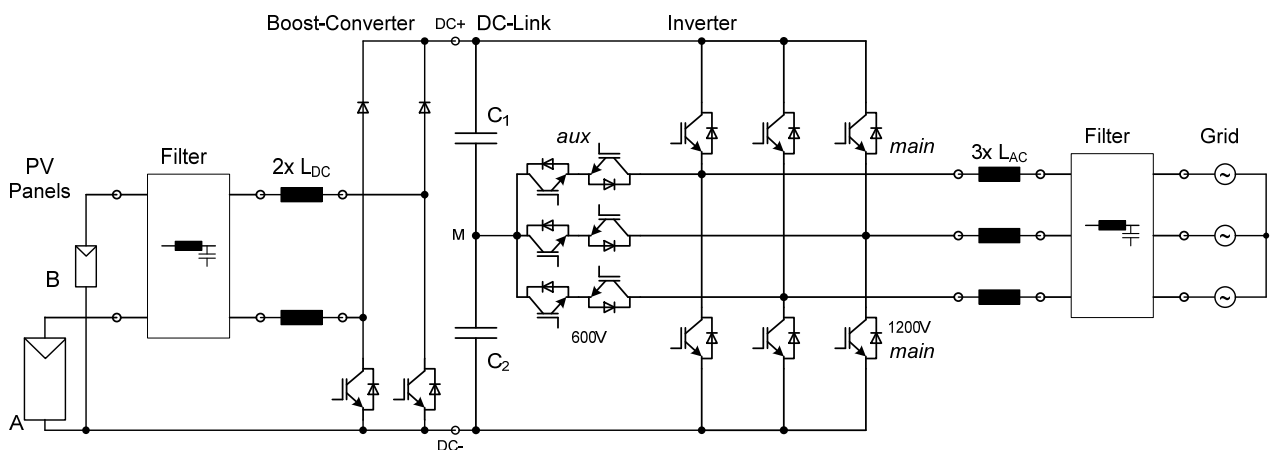


Fig. 2: Circuit diagram of a multi-string PV panel inverter system with transformerless grid-connection

The PV panel input voltages are adapted via boost-converters with DC-chokes L_{DC} to the nominal dc-link voltage of typical $U_{DC,N} = 600$ V up to maximum $U_{DC,max} = 800$ V. Here, the DC-choke's inductance is assumed to $L_{DC} = 9.000$ μ H at chosen IGBTs' switching frequency of $f_s = 16$ kHz. To reduce EMI radiation caused between switching devices in the booster and electrically floating or grounded solar panels, a low-pass filter is inserted.

A three-phase three-level (3L) neutral point clamped (NPC) full bridge inverter (B6I) type 2 converts the DC-link voltage via the *main* 1200V switches. The three phase-shifted PWM-modulated rectangular output pulse voltages feed three AC-chokes L_{AC} . This leads to a sinusoidal inverter output current at grid-frequency $f_{out,N} = 50$ or 60 Hz.

In this example, a nominal inverter output power of $P_N = 17$ kW is chosen. It means an effective output current of $I_{out,N,rms} = 24,5$ A ≈ 25 A at three-phase grid voltage $U_{3AC} = 400$ V. A switching frequency of $f_s = 16$ kHz can be achieved today with the use of 3-Level topology and state-of-the-art Si IGBTs and free-wheeling diodes (FWDs).

The value of the AC-chokes L_{AC} is chosen to obtain a maximum ripple peak-to-peak current $I_{ripple,pp,max}$ of 10% of the nominal output current $I_{out,N,rms}$. In [6] formulas and diagrams to calculate occurring ripple currents are given. In this study an exemplary inductance value of $L_{AC} = 2.500$ μ H is chosen.

Finally, a low-pass filter is inserted between AC-chokes and output terminals to damp residual harmonics above $f_{3dB} = 150$ kHz which is defined in EMI standards for domestic and industrial applications like in EN61000-6-1 and EN61000-6-2. Note, no general EMI standards especially for grid-connected PV solar inverters are existing until now.

Table 1 summarizes the relevant data of the reference system:

Issue	Denomination	Values for a 17kW solar inverter
Heatsink Temperature	T_{hs} [$^{\circ}$ C]	100
Output frequency	$f_{out,N}$ [Hz]	50
Nominal output current	$I_{out,rms,N}$ [A]	25
DC-Link Voltage	U_{DC} [V]	650
Switching frequency	$f_{s,N}$ [kHz]	16
Power factor	$\cos\phi$	1
Nominal output power	$P_{out,N}$ [kW]	17

Table 1: Relevant data of the reference system used in this study

Here, a typical 17 kW PV solar multi-string PV solar inverter with transformerless grid-connection with silicon IGBTs in the booster and 3-Level inverter part has been described. Many PV inverter manufacturers are providing such an inverter topology, and ongoing competition is expected to achieve a significant cost-down of the manufacturing costs. In the following, possible optimizing approaches with SiC devices will be highlighted and discussed.

3 Optimizing approaches for PV power inverter systems

Today, improvements of existing PV inverter systems are mainly linked to a reduction of overall system costs. The efficiency of a PV inverter system is above 98% in all cases and not longer the main focus of development, though a high efficiency is a prerequisite for any successful system. For system cost reduction, a significantly increased switching frequency has been identified as one of the main levers [7]. Here, SiC devices provide an ideal solution with remarkably low switching losses thus maintaining the electrical performance at much higher switching frequency f_s . Aim of this part of the study is to find out how much SiC area has to be spent to achieve 3 times the switching frequency described in Table 1. In this way the inductance of the DC- and AC-chokes can be reduced significantly. All other parameters showed in Table 1 will remain constant. A consideration of overall costs is done based on the technical design.

3.1 Silicon carbide (SiC) JFET module

Silicon carbide is a highly attractive semiconductor material, diodes and switches are superior to standard Si devices in almost all technical aspects. Especially the power losses during switching are reduced significantly, as has been shown for SiC 1200 V JFET half-bridge modules which have been introduced in [2] and will be available soon. In many publications like [4], the technical advantages of SiC JFETs have been shown and discussed.

Here the technical approaches replacing Si IGBTs with SiC JFETs and the gained system benefit will be pointed out.

3.2 Technical approach with SiC semiconductors

Booster part:

The booster reference system is constituted from the Si IGBT modules DF80R12W2H3_B11 [10] and DF160R12W2H3_B11 [11]. The operation switching frequency is $f_s = 16$ kHz at a maximum heatsink temperature of $T_{hs} = 100$ °C. The chip junction operation temperature $T_{vj,op}$ is evaluated with the online simulation tool IPOSIM [5].

The IGBTs in the reference system will be now substituted with a JFET-Solution and the booster's Si FWDs through SiC diodes. With the electrical performance published in [2] the JFET solution achieves a switching frequency of $f_s = 48$ kHz. This leads to an inductance reduction of the booster choke from $L_{DC} = 9$ mH down to $L_{DC} = 3$ mH.

Inverter part:

The inverter reference system is build up in a NPC 2 topology, see Fig. 2. The main switch is a 80 A / 1200 V IGBT High-Speed 3 module in combination with an anti-parallel 1200 V Si FWD. The neutral part of the inverter is realized with a 600 V Si Rapid Diode together with a 600 V IGBT. The maximum operation conditions of this system are described in Table 1.

Fig. 3 shows three technical approaches for the PV inverter part, where only a single half-bridge is shown for clarity.

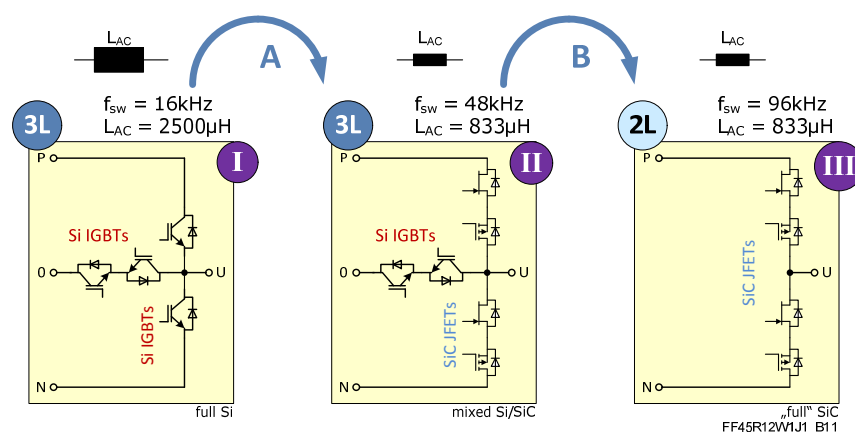


Fig. 3: Optimizing steps of the inverter full-bridge (only single-phase is shown for clarity)

In step A the main 1200 V Si IGBT switches (module I) are replaced by 1200 V SiC JFET devices (module II) to increase switching frequency f_s . With SiC JFET devices providing a nominal current of $I_N = 45$ A a switching frequency of $f_s = 48$ kHz can be achieved. As a consequence of tripled switching frequency, the inductance can be reduced accordingly to one-third while keeping the output ripple current constant. This results in both a smaller and lighter AC choke shrunk from $L_{AC} = 2.500\mu\text{H}$ down to $L_{AC} = 833\mu\text{H}$.

To obtain normally-off behavior during inverter operation the normally-on single switch SiC JFETs are connected in series with low-voltage power p-channel MOSFETs. This cascode configuration [2] ensures safe operation during gate-drive supply power-off and / or detected shoot through. A gate drive chip set especially developed for these JFET / MOSFET cascode enables habitual control of this SiC device [9].

For further system cost reduction also the omission of the IGBT middle leg to get two-level inverter topology 2L is imaginable, see step B and module III in the right of Fig. 3: To obtain the same ripple current at $L_{AC} = 833 \mu\text{H}$ the switching frequency has to be doubled up to $f_s = 96 \text{ kHz}$. For that, a JFET device solution providing 60 A will be necessary. In return, the numbers of needed gate drive units and the complexity of gate control can be reduced.

Table 2 summarizes the different solutions:

Solu- tion	System part	Topology	Module	Semiconductors Fast Commutation part:	$f_{s,max}$ [kHz]	AC- / DC- choke inductanc [μH]	$T_{vj,op}$ main switch [$^{\circ}\text{C}$]
a)	Booster	Booster	DF80R12W2H3_B11 DF160R12W2H3_B11	Full Si: 1200V, 240A HS3 IGBT / FWD	16	9000	150
b)	Booster	Booster	Virtual prototype	Full SiC: 2 x 45A SiC JFET + SiC FWD	48	3000	125
I	Inverter	3-Level NPC 2	Virtual prototype	Full Si: 1200V, 80A HS3 + 600V Rapid FWD	16	2500	150
II	Inverter	3-Level NPC 2	Virtual prototype	SiC: 1200V 45A JFET + 600V SiC Diode	48	833	120
III	Inverter	2-Level	Virtual prototype	Full SiC: 1200V 60A JFET	96	833	130

Table 2: Different solutions for booster and inverter parts. The option to increase the switching frequency leads to lower inductance values of the chokes.

The technical advantages of using SiC devices have been shown. Due to the performance of SiC devices, an optimization of the whole PV inverter system is possible, either by a reduction of total losses, or by increasing the switching frequency. These technical advantages, however, need a translation into total system costs; no technical change will be done without having either a better technical performance, or reduced total system costs.

4 System cost benefit analysis

The costs are modeled for three main components: the power modules, the magnetics and the heat sink. These are the components that are technically linked to the power module itself, and they are the predominant contributors in the cost structure of a PV inverter.

Based on a market research, the costs of magnetic components is found to follow an inverse square-root behavior; upon doubling the switching frequency f_s from 16 kHz to 32 kHz, the costs decline to 70%, while 48kHz will lead to 60% of the initial costs, see the left part of Fig. 4.

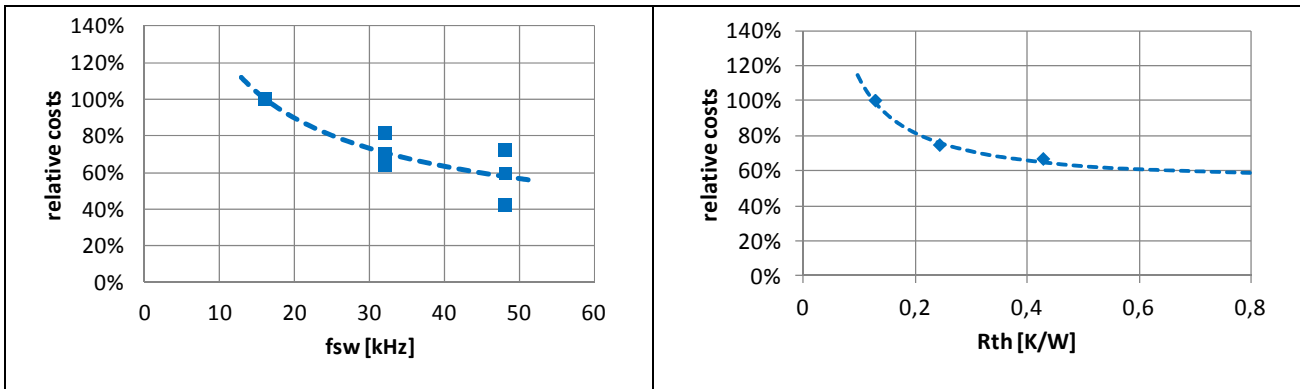


Fig. 4: System costs of magnetic components (left) and heat sink (right) as functions of technical performance.

The heat sink costs are assessed using an Aluminum die-cast process chain model. Main input parameters are the total amount of raw material and the overall dimensions, to cover the dependence on raw material and machine and energy costs. Different heat sink sizes were modeled, and the costs as a function of thermal resistance are given in the right part of Fig. 4. It has to be pointed out that both models are valid within the technical ranges covered in the prior chapter.

Power module prices have been calculated based on certain volume and cost-down scenarios for the SiC JFET switch. In the previous chapter, different technical solutions have been presented, and connections between the topologies, achievable switching frequency f_s and resulting chip junction temperature $T_{vj,op}$ and power dissipation have been established for the booster and inverter part. Together with the cost dependencies presented above, these technical scenarios are converted into respective system costs. These include three main cost drivers for a PV inverter system, namely magnetic components, heatsink, and power modules. In the technical design a constant output power was assumed which leaves the DC-link and other current-carrying components unchanged. These parts together contribute to more than 50% of a typical inverter system. Table 3 gives a summary of the technical solutions considered, and Fig. 5 shows the resulting costs.

Scenario	Booster	Inverter	System Power Losses max:	system costs
1)	IGBT + SiC Diode	3-Level IGBT	732W	100%
2)	SiC JFET + SiC Diode	2-Level SiC JFET	514W	82%
3)	SiC JFET + SiC Diode	3-Level SiC JFET	381W	80%

Table 3: Summary of the technical solutions covered in the cost analysis.

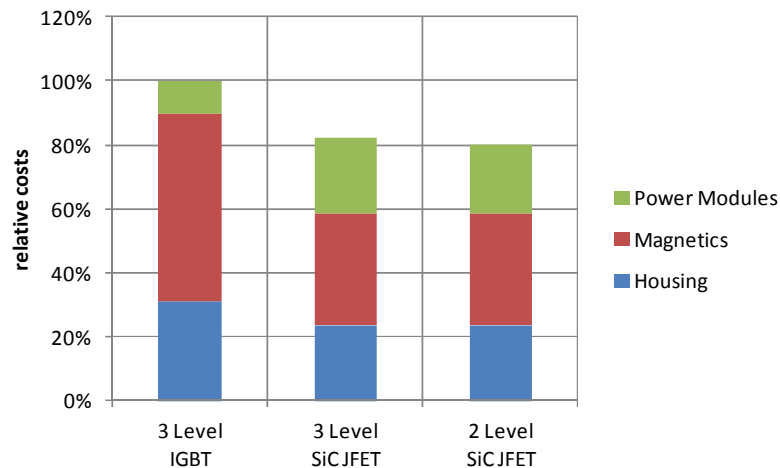


Fig. 5: System costs covering power modules, magnetics and housing for combined inverter and booster solutions as shown. Despite a significant increase in Power module costs, the overall cost reduction is 20%.

Based on the 3-level IGBT solution as reference, a cost reduction of 20% is seen for using SiC devices. The exact savings, of course, depend on the final design parameters of the real system, yet a clear system benefit is recognized in all cases considered here. In the alternative solutions, the savings are similar despite the different technical solution; essentially, savings from an increase in switching frequency f_s and a shrinking of the heatsink as it is modeled here are balanced. In all cases, the expenses for power modules are increasing due to the higher costs for SiC devices, but this is more than compensated by the advantages arising from the superior technical performance: Very low switching losses enable significantly higher f_s and allow for a cost reduction at the magnetics. At the same time, a reduction in total losses offers the possibility to reduce the heat sink with additional cost reduction.

The optimization with respect to the different input parameters is naturally limited by the boundary condition of constant output power. However, changes at this parameter are touching the other system components and are beyond the scope of this paper.

One technical solution to implement SiC devices in PV inverter systems is the 1200 V SiC JFET module FF45R12W1J1_B11 in easyPACK 1B package size [8]. This power module provides 45 A in a 2-level half-bridge topology and can be used to realize a three phase inverter system, or a booster system. The inherent direct drive concept supports the use as a normally-off device [2], [9].

5 Conclusion

In this paper technical solutions have been shown to reduce the system cost of a typical multi-string PV inverter system. In the first part, different implementations using SiC switches are discussed and the impact on main operating parameters like $T_{vj,op}$ and f_s are shown. Cost models are derived for the magnetic components, the heat sink, and the power module itself. These components are predominantly affected by the use of SiC, and at the same time they contribute to a large extent to the overall system costs of a PV inverter. Combining the technical design and operating conditions with the cost models for the components, a cost reduction of 20% is shown for SiC based solutions in comparison to a 3-level Si solution. In both cases, the SiC solutions are shown to be superior despite the higher costs for the power module itself. This is due to the better switching loss performance which enables both higher switching frequency f_s and reduced heat sink size at similar efficiency.

6 References

- [1] Kjaer, S. B.; Pedersen, J. K.; Blaabjerg, F.:
“*A Review of Single-Phase Grid-Connected Inverters for Photovoltaic Modules*”
IEEE Transactions on Industry Applications, Vol. 41, No. 5, September/October 2005
- [2] Domes, D.; Messelke, C.; Kanschat, P.:
“*1st industrialized 1200V SiC JFET module for high energy efficiency applications*”
Conference Proceedings of PCIM 2011, Nürnberg, Germany, 2011
- [3] Franke, W. T., Oestreich, N.; Fuchs, F. W.:
“*Comparison of Transformerless Converter Topologies for Photovoltaic Application Concerning Efficiency and Mechanical Volume*”
IEEE Conference Proceedings of ISIE 2010, Bari, Italy, 2010
- [4] Zhang, X.; Domes, D.; Rupp, R.:
“*Efficiency improvement with SiC based power modules*”
Conference PCIM Europe 2009, Nürnberg, Germany, 2009
- [5] www.infineon.com/IPOSIM
- [6] Kim, H.; Kim, K. - H.:
“*Filter Design for Grid Connected PV Inverters*”
IEEE Conference Proceedings of ICSET 2008, Singapore, Republic of Singapore, 2008
- [7] Hoffmann, S.; Hoene, E.; Zeiter, O.:
“*Electrical, thermal and electromagnetic design of a SiC solar inverter: a case study*”
Conference Proceedings of PCIM 2013, Nürnberg, Germany, 2013
- [8] Infineon Technologies AG
“*Assembly Instructions for the Easy-PressFIT Modules*”
Application Note AN 2009-01 V2.1, Warstein, Germany, April 2013
- [9] Infineon Technologies AG
“*EiceDRIVER™ Enhanced 1EDI30J12Cx*”
Application Note AN2013-17 V2.0, Villach, Austria, December 2013
- [10] Infineon Technologies AG
“*DF80R12W2H3_B11*”
Technical Information V2.0, Warstein, Germany, November 2013
- [11] Infineon Technologies AG
“*DF160R12W2H3_B11*”
Technical Information V2.0, Warstein, Germany, November 2013
- [12] Infineon Technologies AG
“*650V Rapid Diode for Industrial Applications*”
Application Note AN2013-03 V1.0, Villach, Austria, March 2013